

## Improving the Bioactivity of Bioglass/ (PMMA-co-MPMA) Organic/Inorganic Hybrid

R. Ravarian\*, H. Wei\*, F. Dehghani\*

**Abstract**—Binary system of CaO-SiO<sub>2</sub> glasses enables the apatite formation in simulated body fluid (SBF). However, the presence of phosphate content in SiO<sub>2</sub>-CaO-P<sub>2</sub>O<sub>5</sub> glasses leads to the formation of orthophosphate nanocrystalline nuclei, which facilitates the generation of carbonate hydroxyapatite; this compound is more compatible with natural bone. The brittle and less flexible properties of bioactive glasses are the major obstacle for their application as bone implant. The hybridization of essential constituents of bioactive glasses and glass-ceramics with polymers such as PMMA can improve their poor mechanical properties. The aim of this study was to improve the bioactivity of nanocomposites fabricated from poly(methyl methacrylate) (PMMA) and bioglass for bone implant applications. Bioglass compounds with various phosphate contents were used for the preparation of PMMA/bioglass hybrid matrices. Since the lack of adhesion between the two phases impedes the homogenous composite formation, a silane coupling agent such as 3-(trimethoxysilyl)propyl methacrylates (MPMA) was incorporated into the polymer structure. The effect of addition of MPMA on the molecular structure of composite was investigated. Furthermore, the presence of MPMA in the system improved the homogeneity of sample. Increasing phosphate content in the inorganic segment of hybrid up to 10 mol% resulted in the formation of apatite layer on the surface; hence the hybrid was bioactive and suitable candidate for bone tissue engineering.

### I. INTRODUCTION

Biomaterials suitable for bone defect fillers are in demand for orthopaedic applications. Porous bioceramics such as apatites,  $\beta$ -TCP, biphasic ceramics (OHA- $\beta$ -TCP) and bioactive glasses and bioactive glass-ceramics are often used due to their biocompatibility, bioactivity and bonding capability in the body [1]. When implanted in the body, the surface of bioactive materials forms a biologically active hydroxyl carbonate apatite (HCA) layer, which provides the bonding interface with tissues. This HCA phase is chemically and structurally equivalent to the mineral phase in bone, providing interfacial bonding [2]. Sol-gel method is an efficient method for glass production due to the production of high purity, homogeneous glasses, low processing temperatures compared with the melt derived techniques for the glass fabrication. Due to low temperature operating process it is feasible to add organic compounds to the gel during the process [3]. Addition of organic compounds may address brittleness, which is the major obstacle in using bioceramics. Incorporation of organic groups reduces the

degree of crosslinking of inorganic oxide network, which results in more flexible structure.

Polymethyl methacrylate (PMMA) has been widely used for biomedical applications such as prosthetic fixation or as a bone substitute in orthopaedics or in its self curing form in dental prosthetics [4-5]. However, an unresolved problem with using PMMA as a bone substitute is its inertness and lack of bioactivity which leads to the thickening of intervening fibrous tissue layer and the aseptic loosening of implant in some cases [6]. The composites of PMMA with bioactive materials such as calcium phosphates [7] and bioactive glasses [8] are developed to address this issue. Therefore, organic-inorganic hybrids of PMMA and bioactive glass were considered as a suitable biomaterial in this study. The lack of adhesion between two phases (ceramic and polymer) leads to an early failure at the interface. Rhee *et. al* used a silane coupling agent to improve the adhesion between ceramic fillers and PMMA [9]. The mechanical properties of organic-inorganic hybrid materials are strongly dependent on the micro- and nanostructures, but also on the intensity of interactions between organic and inorganic components.

Ohtuski *et. al* investigated the effective parameters on the bioactivity of glasses. They concluded that silanol groups and calcium ions are essential constituents to show bioactivity [10]. Vallet-regi *et al.* found that although the presence of P<sub>2</sub>O<sub>5</sub> in the composition retards the initial reactivity of glasses, it accelerates the growth and size of apatite crystals in the new layer when calcium phosphate nuclei were formed [11].

In this study, PMMA/bioglass hybrids were prepared through sol-gel method to fabricate a bone substitute material with superior properties. Copolymer was hydrolysed and co-condensed with bioglass solution with the presence of HCl as a catalyst for sol-gel reaction. The effects of phosphate groups on the bioactivity of hybrid material and silane coupling agent on the molecular structure of polymer were investigated. Fabricated hybrid may have potential as a bone substitute material due to improved mechanical properties, homogeneity and bioactivity.

### II. MATERIALS AND METHODS

#### A. Synthesis of PMMA-co-MPMA

Poly (methyl methacrylate)-co-3-(trimethoxysilyl)propyl methacrylate (PMMA-co-MPMA) copolymer was prepared by free radical polymerization using

Manuscript received April 14, 2011.

\*: The University of Sydney, School of Chemical and Biomolecular engineering, Sydney, Australia. roya.ravarian@sydney.edu.au

azobisisobutyronitrile (AIBN) as an initiator. MMA ( $4.8 \times 10^{-2}$  mol), MPMA ( $9.6 \times 10^{-4}$  mol) and AIBN ( $2.4 \times 10^{-4}$  mol) were dissolved in 20 mL N,N'-dimethylformamide (DMF). A Schlenk flask with a magnetic stirrer and a rubber septum was charged with the solution of initial chemicals and was degassed by three freeze-pump-thaw cycles. The flask was sealed followed by immersing the flask into an oil bath preheated at 70°C to polymerize. After reaction for 24 h, the flask was taken away from the bath and the reaction mixture was cooled to room temperature followed by precipitation in Diethyl ether. The product was filtered and dried in vacuum.

### B. Preparation of inorganic solution

Inorganic solution was prepared by mixing tetraethylorthosilicate (TEOS), water and calcium nitrate tetrahydrate (CNT) in the molar ratio of TEOS:water:HCl:Ca:NT=1:8:0.01:0.15. Different molar ratios of triethylphosphate (TEP) were added to the inorganic solution to evaluate the effect of phosphate in the bioactivity of product.

### C. Organic-inorganic hybrid products

Copolymer of PMMA-co-MPMA was dissolved in THF (polymer: THF = 10:1 wt.%) and mixed with inorganic solution (IS). For convenience in this paper the combination of organic-inorganic compounds is referred to as C; C0-0 is a solution with 0 mol% TEP and 0 day incubated in SBF. To keep the structure of hybrid, it was slowly dried for a period of one week at room temperature, followed by drying at 37°C for the same period and 48 h at 40°C under vacuum.

### D. In-vitro bioactivity assessment

*In vitro* studies were carried out by soaking the samples in SBF at 37°C for 0, 7 and 14 days. After soaking, the powder was filtered, rinsed with distilled water, and dried at room temperature before analysis by FTIR, XRD and SEM.

### E. Characterization

The synthesized polymer was characterized by  $^1\text{H}$  NMR on a Bruker Ultra Shield Avance (400 MHz) spectrometer using  $\text{CDCl}_3$  as the solvents. The functional groups of samples were analysed by Fourier transform infrared spectroscopy (FTIR; Varian 660-IR) before and after incubation in SBF. X-ray diffractometer (XRD; Shimadzu S6000) with voltage 40 KV and current 30 mA was used to characterize the samples. The surface microstructures and crystal phase formed on the specimens were analysed by field emission scanning electron microscopy (FE-SEM; Zeiss ULTRA plus). This instrument was equipped with Bruker XFlash 4010 EDS detector with high speed acquisition and hypermapping capability.

## III. RESULTS AND DISCUSSION

The molecular structure of synthesized polymer is illustrated in Fig. 1a. As depicted in Fig. 2,  $^1\text{H}$  NMR spectrum in  $\text{CDCl}_3$  and FTIR results confirmed the

structure of synthesized copolymer of PMMA-co-MPMA. Characteristic vibration bands of synthesized polymer are observed in the FTIR spectra; symmetric vibrations at 2892  $\text{cm}^{-1}$  and asymmetric vibrations at 2950  $\text{cm}^{-1}$  are attributed to C-H bonds in  $\text{CH}_3$  [11-12]. Bands at 1734  $\text{cm}^{-1}$  and 1452  $\text{cm}^{-1}$ , were assigned to a C=O bond and  $\text{CH}_2$  bending, respectively. The broad peak detected at 1200-1000  $\text{cm}^{-1}$  is attributed to the overlapping of Si-O-C bending vibrations at around 1088  $\text{cm}^{-1}$  [13] and C-O vibrations at 1150  $\text{cm}^{-1}$  [12]. The typical symmetric vibrations of Si-O bonds at 810-790  $\text{cm}^{-1}$  can also be detected [11].

The characteristic vibrations of inorganic segments were compared with the polymeric segment in Fig. 3. Peaks located at 980  $\text{cm}^{-1}$ , 1029  $\text{cm}^{-1}$  and 1080  $\text{cm}^{-1}$  confirms the presence of Si-O-Si bonds which confirms the network structure of bioglass [14]. The peaks at 1420  $\text{cm}^{-1}$  and 1322  $\text{cm}^{-1}$  are attributed to the  $\text{CO}_3$  and  $\text{NO}_3$  groups in the structure of bioglass, respectively [15-16].

PMMA-co-MPMA copolymer is conjugated to the bioglass structure and form a new composite material. The FTIR result of hybrid (C0-0) depicted in Fig. 3 demonstrates two significant features:

1. The absence of peaks for the polymer (e.g. 1734  $\text{cm}^{-1}$  for C=O bond) may be due to its hydrophobic properties, which resulted in its aggregation and forming second phase in water, which contains inorganic segments of the bioglass structure. This phenomenon is commonly observed for self-assembly molecules [17]. In these structures, after self-assembly, the hydrophobic internal component, which forms the core, is not detected in  $^1\text{H}$  NMR and FTIR analyses.

2. The characteristic peak of Si-O-Si at 1029  $\text{cm}^{-1}$  is significantly changed in the composite material. As depicted in Fig. 3, a broad peak was found for the bioglass system (B0-0); however, a sharp peak was observed for hybrid (C0-0). This variation may be due to the interaction between bioglass and MPMA segment.

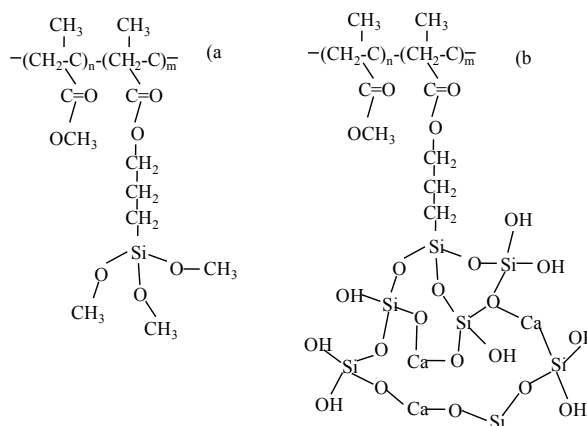


Fig 1. Schematic molecular structure of the a) copolymer PMMA-MPMA, b) copolymer conjugated to the bioglass network.

The homogenous distribution of polymer particles in bioglass solution was investigated by Energy-dispersive X-ray spectroscopy (EDS) analysis. The hybrid sample after

14 days incubation in SBF (sample C0-14) was analysed with EDS. As shown in Fig. 4, all the elements C, Si, and Ca were distributed homogeneously on the surface. The presence of Si and C on the surface was due to the small thickness of the formed calcium phosphate layer, underlining that the penetration depth of emitted X-ray beam was more than the thickness of apatite layer on the sample.

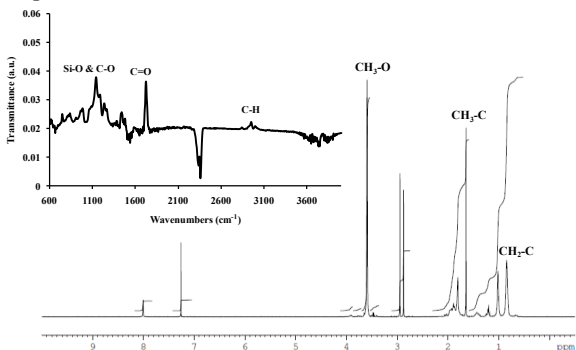


Fig 2.  $^1\text{H}$  NMR of the copolymer PMMA-co-MPMA; Insets is the FTIR results of the synthesized copolymer.

The presence of phosphorous in the hybrid network was evaluated by the characteristic peak at  $800\text{ cm}^{-1}$ . As depicted in Fig. 5, this peak is gradually increased in width by enhancing the phosphorous content in bioglass structure. Two broad peaks in the range of  $900\text{--}970\text{ cm}^{-1}$  and  $1000\text{--}1100\text{ cm}^{-1}$  are attributed to  $\text{PO}_4^{3-}$  symmetric and asymmetric stretch vibrations, respectively [16].

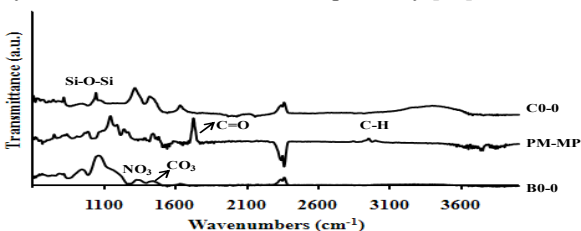


Fig 3. FTIR results of the bioglass without phosphate content (B0-0) and the synthesized polymer (PM-MP) and hybrid materials prepared from combination of organic and inorganic compounds (C0-0)

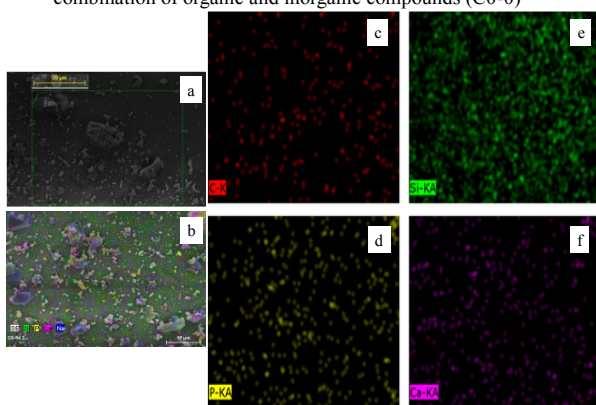


Fig 4. EDS results of the hybrid sample after 14 days incubation in SBF; a) SEM image, b) The colorful map of the specified elements, c) map of carbon content, d) map of phosphorus content, e) map of silicon content, f) map of calcium content

In order to investigate the effect of phosphate content on the *in vitro* bioactivity of composite, hybrid sample was

incubated in SBF for different periods of 7 and 14 days. It can be seen in Fig. 6 that as a function of conditioning time in SBF the spectra for hybrid material showed an increase in the absorbance of phosphate peak in the range of  $1000\text{--}1100\text{ cm}^{-1}$  which is attributed to asymmetric stretch of  $\text{PO}_4^{3-}$  group.

The layer formed on the surface of hybrid samples was analyzed. Two characteristic peaks of phosphate groups ( $1050\text{ cm}^{-1}$ ) and nitrate groups ( $1322\text{ cm}^{-1}$ ) were selected and the ratio of intensities of these two peaks were calculated and demonstrated in Fig. 7. By increasing the phosphate content from 0 mol% up to 5 mol% no significant difference is obtained; however, by increasing the phosphate content up to 10 mol%, the ratio of intensities grows significantly. It means that the presence of phosphate in the system improved the formation of apatite layer on the surface. It should be considered that these data represent the samples which were incubated in SBF for 14 days. This period is sufficient for apatite crystals to form and grow in the appropriate environment of SBF.

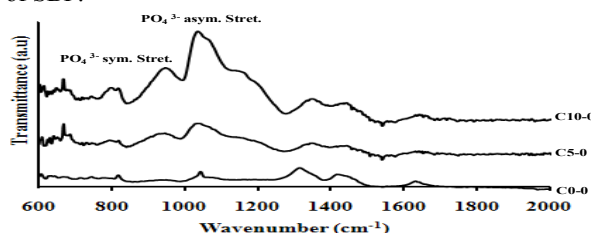


Fig 5. FTIR results of the samples with 0 mol %  $\text{P}_2\text{O}_5$  (C0-0), 5 mol%  $\text{P}_2\text{O}_5$  (C5-0) and 10 mol%  $\text{P}_2\text{O}_5$  (C10-0) before incubation in SBF

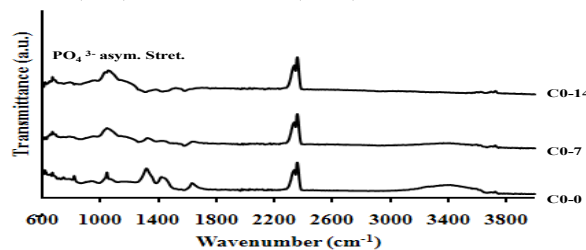


Fig 6. Effect of incubation time in SBF on the formation of phosphate group bands in the hybrid material

Bioactivity assessment was conducted by comparing the morphology and composition of hybrid surface. It was concluded from FTIR and EDS results that the composition of surface layer formed was calcium phosphate. As depicted in Fig. 8 and Fig. 9, the SEM images of samples show the formation of spherical particles on surface.

It was confirmed with SEM results that by increasing the incubation time in SBF, apatite layer formed on the surface was enhanced as depicted in Fig. 7. The effect of phosphate content on the bioactivity of hybrid material was studied. As depicted in Fig. 8, by increasing phosphate content from 0 mol% to 10 mol% the apatite layer on the surface was enhanced. This effect was due to dissolution of phosphate ions in the surrounding fluid and the subsequent formation of an apatite-like layer on the surface. However, at above 10 mol% phosphate ion gel was not formed on the

surface even after two weeks drying at room temperature and 2 weeks in 37°C.

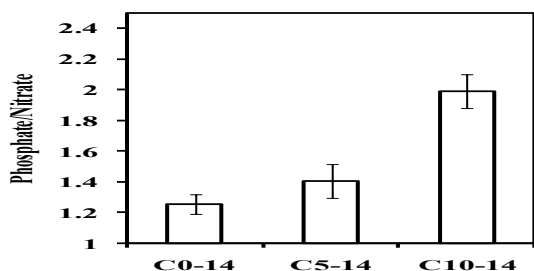


Fig. 7. Semiquantitative analysis (ratio of phosphate peak at 1050  $\text{cm}^{-1}$  to the nitrate peak at 1322  $\text{cm}^{-1}$ ) after 14 days incubation in SBF

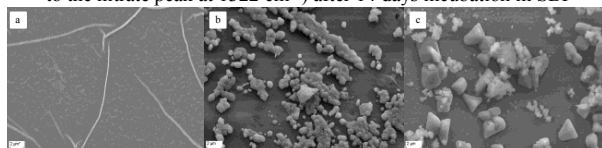


Fig. 8. SEM images of hybrid samples with 0 mol%  $\text{P}_2\text{O}_5$ , a) 0 day (C0-0), b) 7 days (C0-7), c) 14 days (C0-14) incubation in SBF

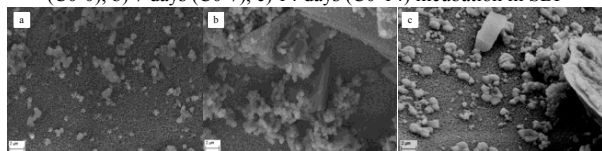


Fig 9. SEM images of hybrid samples with a) 0 mol% (C0-14), b) 5 mol % (C5-14) and c) 10 mol % (C10-14)  $\text{P}_2\text{O}_5$

The formation of apatite layer over the samples with different amount of phosphate ion was confirmed by XRD analysis which is shown in Fig. 10. Peaks assigned to hydroxyapatite with low crystallinity are observed at about 26° and 32° after soaking for 14 days.

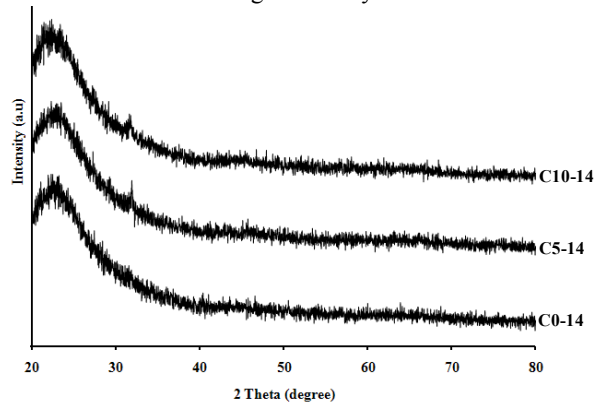


Fig. 10. XRD results for hybrid samples with 0 mol %, 5 mol % and 10 mol%  $\text{P}_2\text{O}_5$  after 14 days incubation in SBF

#### IV. CONCLUSIONS

The nanocomposite of PMMA-co-MPMA and bioglass was prepared via sol-gel method which enables the fabrication of hybrid at room temperature. In this method, PMMA-co-MPMA chains are entrapped into the gel-like structure of bioglass. The presence of (MPMA) improved the homogeneity and attachment of copolymer to inorganic segment in the hybrid. The results of *in vitro* study demonstrate that increasing the concentration of phosphate in bioglass promotes the apatite formation on the surface

of composite samples. However, above 10%, the formation of apatite layer was impeded due to substantial pH increase in medium. It is anticipated that the nanocomposites produced in this study have high potential for bone implant applications.

#### REFERENCES

- [1] Arcos, D., C.V. Ragel, and M. Vallet-Regi, *Bioactivity in glass/PMMA composites used as drug delivery system*. *Biomaterials*, 2001. **22**(7): p. 701-708.
- [2] Rezwani, K., Q.Z. Chen, J.J. Blaker, and A.R. Boccaccini, *Biodegradable and bioactive porous polymer/inorganic composite scaffolds for bone tissue engineering*. *Biomaterials*, 2006. **27**(18): p. 3413-3431.
- [3] Jones, S.M., S.E. Friberg, and J. Sjöblom, *A bioactive composite material produced by the sol-gel method*. *J. Mater. Sci.*, 1994. **29**(15): p. 4075-80.
- [4] J.F. Orr, N.J.D., *Measurement of Shrinkage Stresses in PMMA Bone Cement*. *Applied Mechanics and Materials*, 2004. **1-2**: p. 127-132.
- [5] Kosuge, Y., *Influence of PMMA powder on properties of MMA-TBB resin cement*. *Shika Zairyo, Kikai*, 2000. **19**(1): p. 92-101.
- [6] Ferreira, B.J.M.L., M.G.G.M. Duarte, M.H. Gil, R.N. Correia, J. Roman, and M. Vallet-Regi, *In vitro bioactivity in glass-ceramic / PMMA-co-EHA composites*. *Key Eng. Mater.*, 2004. **254-256**(Bioceramics): p. 581-584.
- [7] Beruto, D.T., S.A. Mezzasalma, M. Capurro, R. Botter, and P. Cirillo, *Use of  $\alpha$ -tricalcium phosphate (TCP) as powders and as an aqueous dispersion to modify processing, microstructure, and mechanical properties of polymethylmethacrylate (PMMA) bone cements and to produce bone-substitute compounds*. *J. Biomed. Mater. Res.*, 2000. **49**(4): p. 498-505.
- [8] Okada, Y., K. Kawanabe, H. Fujita, K. Nishio, and T. Nakamura, *Repair of segmental bone defects using bioactive bone cement: Comparison with PMMA bone cement*. *J. Biomed. Mater. Res.*, 1999. **47**(3): p. 353-359.
- [9] Rhee, S.-H., J.-Y. Choi, and H.-M. Kim, *Preparation of a bioactive and degradable poly( $\epsilon$ -caprolactone)/silica hybrid through a sol-gel method*. *Biomaterials*, 2002. **23**(24): p. 4915-4921.
- [10] Ohtsuki, C., T. Miyazaki, and M. Tanihara, *Development of bioactive organic-inorganic hybrid for bone substitutes*. *Mater. Sci. Eng., C*, 2002. **C22**(1): p. 27-34.
- [11] Manzano, M., A.J. Salinas, and M. Vallet-Regi, *P-Containing ORMOSILS for bone reconstruction*. *Prog. Solid State Chem.*, 2006. **34**(2-4): p. 267-277.
- [12] Hosseinalipour, S.M., A. Ershad-langroudi, A.N. Hayati, and A.M. Nabizade-Haghighi, *Characterization of sol-gel coated 316L stainless steel for biomedical applications*. *Prog. Org. Coat.*, 2010. **67**(4): p. 371-374.
- [13] Varma, I.K., A.K. Tomar, and R.C. Anand, *Copolymerization of  $\gamma$ -methacryloxypropyltrimethoxysilane and methyl methacrylate*. *J. Appl. Polym. Sci.*, 1987. **33**(4): p. 1377-88.
- [14] Costa, H.S., E.F.B. Stancioli, M.M. Pereira, R.L. Orefice, and H.S. Mansur, *Synthesis, neutralization and blocking procedures of organic/inorganic hybrid scaffolds for bone tissue engineering applications*. *J. Mater. Sci. Mater. Med.*, 2009. **20**(2): p. 529-535.
- [15] Vivekanandan, K., S. Selvasekarapandian, and P. Kolandaivel, *Raman and FT-IR studies of  $\text{Pb}_4(\text{NO}_3)_2(\text{PO}_4)_2 \cdot 2\text{H}_2\text{O}$  crystal*. *Mater. Chem. Phys.*, 1995. **39**(4): p. 284-9.
- [16] Aguiar, H., J. Serra, P. Gonzalez, and B. Leon, *Structural study of sol-gel silicate glasses by IR and Raman spectroscopies*. *J. Non-Cryst. Solids*, 2009. **355**(8): p. 475-480.
- [17] Wei, H., X.-Z. Zhang, Y. Zhou, S.-X. Cheng, and R.-X. Zhuo, *Self-assembled thermoresponsive micelles of poly(*N*-isopropylacrylamide-*b*-methyl methacrylate)*. *Biomaterials*, 2006. **27**(9): p. 2028-2034.